

A lasso-alternative to Dijkstra’s algorithm for identifying short paths in networks

Anqi Dong*

Amirhossein Taghvaei†

Tryphon T. Georgiou‡

December 1, 2025

Abstract

We revisit the problem of finding the shortest path between two selected vertices of a graph and formulate this as an ℓ_1 -regularized regression – Least Absolute Shrinkage and Selection Operator (lasso). We draw connections between a numerical implementation of this lasso-formulation, using the so-called LARS algorithm, and a more established algorithm known as the bi-directional Dijkstra. Appealing features of our formulation include the applicability of the Alternating Direction of Multiplier Method (ADMM) to the problem to identify short paths, and a relatively efficient update to topological changes.

Keywords: Graph Theory, static optimization problems, routing algorithms, control over networks, transportation.

1 Introduction

The problem of finding the shortest path between two vertices of a graph has a long history [19, 24] and a wide range of applications [14, 23]. A classical algorithm to determine a shortest path is due to Dijkstra [10]. Since Dijkstra’s early work, a variety of alternative methods have been developed to reduce complexity and address variants of the problem [2, 4, 8, 12, 22]. A salient issue in applications involving graphs of considerable size, which motivated the present work, is that identifying a shortest path is not absolutely essential, whereas identifying a reasonably short path may suffice [16, 23].

Driven by such considerations and inspired by the effectiveness of convex optimization techniques to address large-scale problems [5, 7], we introduce a formulation of the shortest path problem as an ℓ_1 -regularized regression, known as the *Least Absolute Shrinkage and Selection Operator (lasso)* [20]. This type of regularization/relaxation is ubiquitous in inverse problems throughout engineering, statistics, and mathematics, with a rich library of numerical implementations for high-dimensional problems – an added incentive for the approach that we advocate.

*Division of Decision and Control Systems and Department of Mathematics, KTH Royal Institute of Technology, SE-100 44 Stockholm, Sweden (anqid@kth.se).

†Department of Aeronautics and Astronautics, University of Washington, Seattle, WA 98195, USA (amirtag@uw.edu).

‡Department of Mechanical and Aerospace Engineering, University of California, Irvine, CA 92697, USA (tryphon@uci.edu).

Thus, a main contribution of this work is to formulate the shortest path problem as ℓ_1 -regularized regression, a convex optimization problem [20, 21]. This formulation is, to the best of the authors’ knowledge, original.

A second contribution stems from exploring at depth a popular ℓ_1 -regularized regression solver, known as *Least Angle Regression (LARS)*, as applied to the shortest path problem. Specifically, we have shown (Theorem 8) that the LARS implementation of our “lasso-shortest-path” formulation replicates a defining feature of the so-called *bi-directional Dijkstra algorithm*, to iteratively build two shortest-path trees, starting from the two specified vertices and until the two trees connect. Through this connection, we present a new perspective of Dijkstra’s algorithm that is completely different than the common presentation as a greedy algorithm or a dynamic programming viewpoint [18].

Lastly, we explore the *Alternating Direction of Multiplier Method* (ADMM) [5, 7], and a variant (InADMM) [26], for reducing the computational cost in identifying an approximate shortest path for very large graphs. The benefits of ADMM and its variants include: **(i)** it admits distributed implementation, initialized with any suitable path (*warm-start*), if one is available. Such a feature speeds up convergence, is especially useful when a short path needs to be updated following topological changes in the graph. **(ii)** it can be adopted as a solver for the parallel lasso (19), whereby multiple-pair and all-pair shortest path problems can be considered and formulated in the same manner. The ADMM algorithm proposed here is completely different than earlier proposals on the subject, e.g., the self-stabilizing approach in [8]. The proposed algorithm aims at identifying an (approximate) shortest path between specified vertices, allowing for better computational complexity and relatively efficient updates to topological changes.

The present work builds on our earlier conference publication [11], where we first presented the idea of relaxing the search for a shortest path via ℓ_1 -regularized regression, and pointed out analogies to the bi-directional Dijkstra algorithm. In [11], in particular, we sketched the LARS–Dijkstra connection and illustrated the idea via small synthetic examples. The present work aims to bring out the significance of the approach, sharpen the link between the two viewpoints, and provide detailed streamlined justification of points of contact. To this end, we herein provide detailed analysis of crossing/joining times (in the parlance of the LARS algorithm) and how/when these are manifested in the present setting (Section 4), explore uniqueness of shortest path under both strong and weak regularity assumptions (Section 3), examine scalability, and discuss links to practical Dijkstra implementations from the new perspective (Section 6). A focus in our exposition is on how to capitalize on fast numerical solvers to improve on speed and robustness. In particular, we detail insights in utilizing proximal lasso solvers (ADMM and an inexact variant based on sparse Cholesky and preconditioned conjugate gradients, including warm starts, over-relaxation, and stopping criteria). We report results on image grids, road networks, and random geometric graphs at scales from 10^3 to 10^4 nodes, with all parameters listed for reproducibility (Section 6).

The outline of the work is as follows. Section 2 introduces notation along with basic concepts and a brief account of Dijkstra’s algorithm. Section 3 casts the search for short paths in a network as a convex optimization problem as discussed. Section 4 details the algorithmic steps for updating state-values on edges, that turn out to coincide with the so-called *lasso solution* in the LARS algorithm. Section 5 highlights the commonality of features between the LARS algorithm and bi-directional Dijkstra algorithm. Finally, Section 6 explores the application of the ADMM method to our lasso formulation, and highlights its relevance in identifying short, but not necessarily shortest, paths in very large graphs.

2 Preliminaries

2.1 Graph theoretic notations and definitions

Throughout, we consider a weighted *undirected* graph \mathcal{G} that is connected and has no self-loops or multi-edges. We write $\mathcal{G} = (\mathcal{V}, \mathcal{E}, \mathcal{W})$, where $\mathcal{V} = \{v_1, \dots, v_n\}$ is the set of vertices/nodes, $\mathcal{E} = \{e_1, \dots, e_m\}$ is the set of edges, and $\mathcal{W} = \{w_1, \dots, w_m\}$ a set of weights corresponding to the edges. We will consistently use $n = |\mathcal{V}|$ and $m = |\mathcal{E}|$ for the cardinality of these two sets. When labeling edges, we also use the notation (v_i, v_j) for the edge that connects vertices v_i and v_j , without significance to the order.

However, as is common, in defining the *incidence matrix* of the graph, denoted by $D(\mathcal{G})$ an arbitrary but fixed orientation is assigned to edges that has no bearing on the results. To this end, the incidence matrix is defined as the $n \times m$ matrix with (i, j) th entry

$$[D]_{ij} = \begin{cases} +1 & \text{if the } i\text{th vertex is the tail of edge } e_j, \\ -1 & \text{if the } i\text{th vertex is the head of edge } e_j, \\ 0 & \text{otherwise.} \end{cases}$$

It is convenient to define the *weight matrix* $W = \text{diag}(w_1, \dots, w_m)$ as the diagonal matrix formed by the weights in \mathcal{W} , consistent with the ordering in \mathcal{E} .

A path from vertex v_s to vertex v_t is a sequence of connected edges

$$p = \{(v_{i_0}, v_{i_1}), (v_{i_1}, v_{i_2}), \dots, (v_{i_{\ell-1}}, v_{i_\ell})\}$$

that “starts” at $v_{i_0} = v_s$ and “terminates” at $v_{i_\ell} = v_t$. An alternative representation of the path, which now encodes edge-orientation that is consistent with that in specifying D , is in terms of the *incidence vector* $x^{(p)}$. This is an m -dimensional vector defined as follows: the i th entry $(x^{(p)})_i$ is $+1$, or -1 , depending on whether an edge $(v_{i_{k-1}}, v_{i_k})$ (for some $k \in \{1, \dots, \ell\}$) in the path is the i th edge in \mathcal{E} and is listed with orientation consistent or not with the tail/head designation in specifying D , respectively; if the i th edge is not in the path, $(x^{(p)})_i = 0$. The *length of the path* is defined as the sum of edge-weights, i.e.,

$$\text{length}(p) \triangleq \sum_{e_i \in p} w_i = \|Wx^{(p)}\|_1,$$

where $\|\cdot\|_1$ denotes the ℓ_1 -norm.

A connected graph is said to be a *tree* if it has no cycle, i.e., it has no path where $s = t$. If \mathcal{G} is connected, there is always a subgraph which is a tree. When \mathcal{G} is a tree, $m = n - 1$ and there is a unique path from any given vertex to any other. Any vertex can be designated as *root*, and the structure of graph is encapsulated by all paths connecting vertices to the root ($n - 1$ paths). The $(n - 1) \times (n - 1)$ matrix of incidence vectors of all such paths is referred to as *path matrix* (often with reference to the root) and denoted by P_{v_1} , or simply P , when the root is clear from the context. Interestingly, P is closely connected to the incidence matrix D . This is the content of the following lemma, which is key for results in Section 5 but also of independent interest.

Lemma 1. *Let \mathcal{G} be a tree rooted at v_1 with n vertices and P its path matrix. The pseudoinverse of its incidence matrix D , denoted as D^+ , is ¹*

$$D^+ = \begin{bmatrix} -\frac{1}{n}P\mathbb{1}_{n-1}, & PJ \end{bmatrix},$$

¹Throughout, $\mathbb{1}_k$ denotes the k -column vector with entries equal to 1, and I_k the $k \times k$ identity matrix.

where $J = (I_{n-1} - \frac{1}{n} \mathbb{1}_{n-1} \mathbb{1}_{n-1}^T)$.

Proof. See [3, Theorem 2.10 & Lemma 2.15]. □

2.2 Shortest path problem and Dijkstra's algorithm

Let $\mathcal{P}_{s,t}$ denote the set of all paths between v_s and v_t . This set is non-empty because the graph is connected. The shortest path problem is to find a path with minimum length over all the paths between v_s and v_t , i.e.,

$$\arg \min_{p \in \mathcal{P}_{s,t}} \text{length}(p). \quad (1)$$

The minimum value is known as the *distance* between v_s and v_t . A well-known search algorithm - Dijkstra's algorithm, has been proposed for this problem.

Dijkstra's algorithm [10] begins with the "starting" vertex v_s , and initially assigns a distance of 0 to v_s and $+\infty$ to all other vertices. It iteratively labels the vertex with the lowest *distance estimate* as *visited* and updates the distance estimates of its neighbors that have not yet been visited (*unvisited*). The distance estimates are updated by summing up the distances of visited vertices and the weights of the edges linking these vertices to their unvisited neighbors. Dijkstra's algorithm terminates when v_t is visited and produces the shortest path from source vertex v_s to others vertices in the form of shortest-path tree.

The essential feature of Dijkstra's algorithm is that it iteratively constructs the shortest-path tree rooted at v_s to all the visited vertices before reaching the target v_t . Similarly, bi-directional Dijkstra algorithm constructs two shortest-path trees rooted at v_s and v_t and terminates when the two trees connect.

Later on in Section 5, we will point out analogies between the bi-directional Dijkstra algorithm and properties of the LARS algorithm applied to the shortest-path problem advocated herein.

3 Linear programming formulation

We now cast the shortest path problem (1) as a linear program. To this end, we will use a well-known technique for finding sparse solutions to linear equations by minimizing the ℓ_1 norm of a vector as a surrogate for the count of its non-vanishing entries [20].

In our setting, constraints are expressed in terms of D (incidence, also constraint matrix) and x , the incidence vector of a sought path p from v_s to v_t , in that,

$$p \in \mathcal{P}_{s,t} \quad \Rightarrow \quad Dx^{(p)} = y^{(s,t)}. \quad (2)$$

Here, $y_i^{(s,t)} = \mathbf{1}_{\{s\}} - \mathbf{1}_{\{t\}}$ is the *indicator vector* in \mathbb{R}^n of a *virtual edge* directly connecting v_s to v_t ; the path together with the virtual edge form a *closed cycle*. Throughout, $\mathbf{1}_{\{\cdot\}}$ denotes the indicator function of set $\{\cdot\}$. Note that linear combinations $x = ax^{(p_1)} + (1-a)x^{(p_2)}$ with $a \in (0,1)$ of incidence vectors of two distinct paths p_1 and p_2 between v_s and v_t , also satisfy the constraint $Dx = y^{(s,t)}$. That is, although an exact correspondence between the two sides of (2) does not hold, it does hold between the *shortest path* and a corresponding integer vertex of the polytope defined by the constraint matrix D . Thus, we *propose*

$$\arg \min_{x \in \mathbb{R}^m} \|Wx\|_1, \quad \text{s.t.} \quad Dx = y^{(s,t)} \quad (3a)$$

as a way to solve the shortest path problem.

To gain insight as to the nature of the minimizer, problem (3a) can be recast as the linear program:

$$\arg \min_{\xi \geq 0} \sum_{i=1}^m w_i (x_i^+ + x_i^-), \quad \text{s.t.} \quad \mathcal{D}\xi = y^{(s,t)} \quad (3b)$$

with $\mathcal{D} := [D, -D]$ and $\xi \in \mathbb{R}^{2m}$. The solutions to (3a) and (3b) correspond via $\xi = \begin{bmatrix} x^+ \\ x^- \end{bmatrix} \geq 0$, where x_+ (x_- , resp.) is the vector of positive (negative, resp.) entries of x , setting zero for the negative (positive, resp.) entries, i.e.,

$$x^+ := \max(x, 0), \quad x^- := \max(-x, 0), \quad x = x^+ - x^-, \quad \text{and} \quad |x| = x^+ + x^-.$$

The constraint matrix \mathcal{D} in (3b) is *totally unimodular* (i.e., all minors have determinant in $\{0, \pm 1\}$) [3, Lemma 2.6], and therefore, application of [1, Theorem 11.11 (Unimodularity Theorem)] guarantees that there exists an integral optimal solution; if the shortest path is unique, then the optimal solution is unique and $\{0, \pm 1\}$ -valued. Thus, x in (3a) corresponds to a valid incidence vector.

3.1 Lasso formulation

Returning to (3a), rewritten in the form

$$\arg \min_{\beta} \left\{ \|\beta\|_1 \mid \|Q\beta - y\|_2^2 = 0 \right\} \quad (3a')$$

in new variables $\beta = Wx$, $y = y^{(s,t)}$, and $Q = DW^{-1}$, leads us a relaxation as the ℓ_1 -regularized regression

$$\beta(\lambda) := \arg \min_{\beta \in \mathbb{R}^m} \frac{1}{2} \|y - Q\beta\|_2^2 + \lambda \|\beta\|_1, \quad (4)$$

with (regularization parameter) $\lambda > 0$. The formulation (4) is known as *lasso* [21].

The limit $\beta_0 := \lim_{\lambda \rightarrow 0} \beta(\lambda)$ from (4), for $\lambda > 0$, provides the indicator vector $\mathbf{x}_0 = W^{-1}\beta_0$ of a path under uniqueness and regularity (non-degeneracy) of the shortest path. Under these conditions, there exists $\bar{\lambda} > 0$ such that $\text{supp}(\beta(\lambda)) = \text{supp}(\beta_0)$ for all $\lambda \in (0, \bar{\lambda})$. For $\lambda > 0$, $\beta(\lambda)$ may not correspond to a path. However, due to continuity and the fact that \mathbf{x}_0 in the limit must be $\{0, \pm 1\}$ -valued, for sufficiently small λ , $\mathbf{x}(\lambda) = W^{-1}\beta(\lambda)$ reveals the shortest path (e.g., by rounding the values to the nearest integer). In practice, applying a small threshold to $\mathbf{x}(\lambda)$ followed by a connectivity check reliably recovers the path.

Thus, the lasso formulation represents a viable and attractive approach for solving the shortest path problem. Interestingly, as we show in Section 5, the LARS algorithm – a popular solver for lasso (4), shares features of the bi-directional Dijkstra algorithm. Most importantly, the lasso formulation (4), as discussed in Section 6, allows the use of proximal optimization methods for obtaining satisfactory approximations of the shortest path in large graph settings.

3.2 Uniqueness of the lasso solution

A sufficient condition for uniqueness of solution to (4) is that $\text{rank}(Q) = m$, the size of β and number of edges [21, Lemma 2]. However, recall that $WQ = D$, the incidence matrix. It follows that $\text{rank}(Q) = m$ only holds when the graph is a tree (or possibly, a disjointed set of trees,

cf. [3, Theorem 2.3]). Evidently, such an assumption is too restrictive, also since the shortest path problem in this case becomes trivial.

Herein, we introduce a fairly general sufficient condition for the uniqueness of solution to (4) (as we claim next), that is in fact generic, for generic weights.

Assumption 1 (Strong (terminal-to-all) uniqueness). *The shortest path between vertex v_s and any other vertex is unique, and the same applies to v_t .*

We note that $\beta(\lambda)$ from (4) turns out to be piece-wise linear (see Section 4). The values of λ where the slope changes are referred to as *breakpoints*. With this in place, the implications of the assumption to our problem can be stated as follows.

Lemma 2 (Uniqueness). *Under Assumption 1, Problem (4) admits a unique solution for all $\lambda > 0$.*

It is important to note, in general, that the quadratic expression in (4) may not be strictly convex – when $\text{rank}(Q) \leq n - 1 < m$, Q has a nontrivial null space, whereas on trees where $\text{rank}(Q) = m$, strict convexity is ensured. The key idea in proving uniqueness under the conditions of the lemma requires a discussion of the LARS algorithm that is explained next. Hence the proof is deferred to Appendix C.

Assumption 2 (Weak (s - t) uniqueness). *The shortest s - t path is unique, whereas shortest paths from s (or from t) to other vertices may be non-unique.*

Remark 1 (Consequences under Assumption 2). *Under Assumption 2, problem in (4) has a minimizer for every $\lambda > 0$. For almost all λ the minimizer is unique. Non-uniqueness can occur only at parameter values where ties create multiple geodesics from s or t to intermediate vertices. At such values, LARS may admit simultaneous edge arrivals and the active set can exhibit crossings.*

4 The LARS algorithm

4.1 Karush-Kuhn-Tucker (KKT) conditions

The solution $\beta(\lambda)$ of (4) must satisfy the *KKT condition* [21, Section 2.1]

$$Q^T(y - Q\beta(\lambda)) = \lambda\gamma, \quad (5)$$

where the vector γ is in the sub-differential of $\|\beta(\lambda)\|_1$, with j th component given by

$$\gamma_j \in \begin{cases} \{\text{sign}(\beta_j(\lambda))\} & \text{if } \beta_j(\lambda) \neq 0, \\ [-1, 1] & \text{if } \beta_j(\lambda) = 0. \end{cases}$$

The KKT condition in (5) motivates us to divide the indices $\{1, 2, \dots, m\}$ into two set: an *active* set (also, *equicorrelation* set [21]) \mathcal{A} and, a *non-active* set \mathcal{A}^c , i.e.,

$$\mathcal{A} \triangleq \{j \mid \beta_j(\lambda) \neq 0\}, \quad \mathcal{A}^c \triangleq \{j \mid \beta_j(\lambda) = 0\}. \quad (6)$$

Let $\beta_{\mathcal{A}}(\lambda)$ denote the vector $\beta(\lambda)$ with the non-active (or equivalently, zero) entries removed and, likewise, $Q_{\mathcal{A}}$ be the matrix Q with the columns corresponding to the non-active set removed, and

thus fully depends on $\beta(\lambda)$. Then, the KKT condition (5) can be expressed as

$$Q_j^T (y - Q_{\mathcal{A}} \beta_{\mathcal{A}}(\lambda)) = s_j \lambda, \quad \forall j \in \mathcal{A}, \quad (7a)$$

$$\left| Q_j^T (y - Q_{\mathcal{A}} \beta_{\mathcal{A}}(\lambda)) \right| \leq \lambda, \quad \forall j \in \mathcal{A}^c, \quad (7b)$$

where Q_j denotes the j th column of Q and the *sign vector*

$$s := \text{sign} \left(Q_{\mathcal{A}}^T (y - Q_{\mathcal{A}} \beta_{\mathcal{A}}(\lambda)) \right) = \text{sign}(\beta_{\mathcal{A}}), \quad (8)$$

with j th element the sign (± 1) of the j th entry of $\beta_{\mathcal{A}}$.

4.2 The LARS algorithm

The LARS algorithm, as formulated in [21, Section 3.1] to solve lasso, finds the *solution path* of $\beta(\lambda)$ that meets the KKT condition (5) for all $\lambda > 0$. The algorithm is initialized with $\lambda_0 = \infty$, $\mathcal{A}_0 = \emptyset$, and $s_0 = \emptyset$. The solution path $\beta_{\mathcal{A}}(\lambda)$, in (9) below, is computed for decreasing λ , and is piece-wise linear and continuous with breakpoints $\lambda_0 > \lambda_1 > \dots > 0$. Breakpoints are successively computed at each iteration of the algorithm, and the linear segment of $\beta_j(\lambda)$ is determined to satisfy the element-wise KKT condition as detailed in (7). As λ crosses breakpoints, the active (non-active) set (6) and the sign vector (8) are updated accordingly.

We now detail the k th iteration of the LARS algorithm, initializing $\lambda = \lambda_k$, $\mathcal{A} = \mathcal{A}_k$, $s = s_k$, and seeking the next breakpoint λ_{k+1} . The lasso variable $\beta_{\mathcal{A}_k}(\lambda)$, as a function of λ , is calculated as the minimum ℓ_2 -norm solution of (7a), and is given by:

$$\beta_{\mathcal{A}_k}(\lambda) = \left(Q_{\mathcal{A}_k}^T Q_{\mathcal{A}_k} \right)^+ \left(Q_{\mathcal{A}_k}^T y - \lambda s_k \right) = a^{(k)} - b^{(k)} \lambda, \quad (9)$$

where $(\cdot)^+$ denotes the Moore–Penrose pseudoinverse² and

$$\begin{aligned} a^{(k)} &:= \left(Q_{\mathcal{A}_k}^T Q_{\mathcal{A}_k} \right)^+ Q_{\mathcal{A}_k}^T y, \\ b^{(k)} &:= \left(Q_{\mathcal{A}_k}^T Q_{\mathcal{A}_k} \right)^+ s_k. \end{aligned} \quad (10)$$

The next breakpoint λ_{k+1} is determined as the largest value at which the KKT condition $(Q_j^T (y - Q_{\mathcal{A}_k} \beta_{\mathcal{A}_k}(\lambda)) = \lambda \gamma_j)$ is violated by λ . Such a violation occurs in two circumstances (“crossing/joining” in the language of [21]), either (7a) or (7b) fails.

i) The “joining” case is when condition (7b) is violated for some $j \in \mathcal{A}_k^c$, i.e.,

$$\left| Q_j^T (y - Q_{\mathcal{A}_k} \beta_{\mathcal{A}_k}(\lambda)) \right| \leq \lambda$$

no longer holds. For each index $j \in \mathcal{A}_k^c$, this happens at $\lambda = t_j^{\text{join}}$ given by

$$t_{j,k}^{\text{join}} = \frac{Q_j^T (Q_{\mathcal{A}_k} a^{(k)} - y)}{Q_j^T Q_{\mathcal{A}_k} b^{(k)} \pm 1}, \quad (11)$$

²Herein, W is positive diagonal and D has full column rank (the incidence on a tree). Then we have $(DW^{-1})^+ = (W^{-1})^{-1} D^+ = W D^+$.

where the choice \pm is the one for which $t_{j,k}^{\text{join}} \in [0, \lambda_k]$. We set “joining time”

$$\lambda_{k+1}^{\text{join}} := \max_{j \in \mathcal{A}_k^c} \left\{ t_{j,k}^{\text{join}} \right\}.$$

ii) The “crossing” case is when condition (7a) is violated for some $j \in \mathcal{A}_k$ so that one of the elements of $\beta_{\mathcal{A}_k}(\lambda)$ crosses zero (changes its sign), i.e. $a_j^{(k)} - \lambda b_j^{(k)} = 0$ for some $\lambda < \lambda_k$. For each index $j \in \mathcal{A}_k$, the crossing happens at $\lambda = t_j^{\text{cross}}$ given by

$$t_{j,k}^{\text{cross}} = (a_j^{(k)} / b_j^{(k)}) \cdot \mathbf{1}_{\{0 < (a_j^{(k)} / b_j^{(k)}) < \lambda_k\}}. \quad (12)$$

We set “crossing time”

$$\lambda_{k+1}^{\text{cross}} = \max_{j \in \mathcal{A}_k} \left\{ t_{j,k}^{\text{cross}} \right\}.$$

The next breakpoint is

$$\lambda_{k+1} = \max \left\{ \lambda_{k+1}^{\text{join}}, \lambda_{k+1}^{\text{cross}} \right\}. \quad (13)$$

If the joining occurs, the joining index is added to the active set, and the sign vector is updated. If a crossing happens, the crossing index is removed from the active set. The overall algorithm is summarized as follows .

Algorithm 1 (LARS algorithm for the lasso (4))

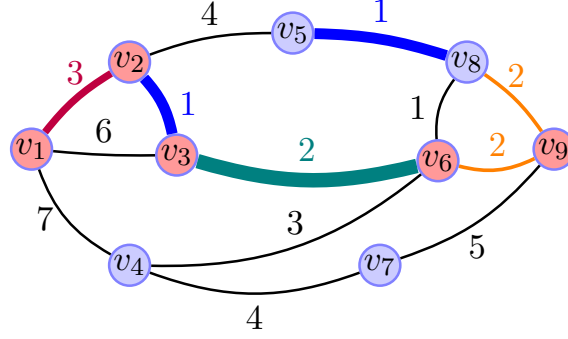
Input: matrix $Q = DW^{-1}$, vector $y = y^{(s,t)}$.

Output: incidence vector $\mathbf{x}_0 = W^{-1}\beta_0$, distance $\|\beta_0\|_1$.

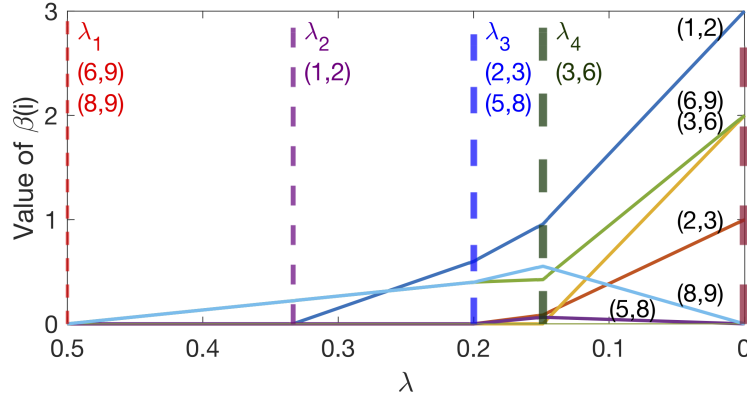
- 1: $k = 0$, $\lambda_0 = \infty$, $\mathcal{A} = \emptyset$, $s = 0$, $a^{(0)} = 0$ and $b^{(0)} = 0$.
 - 2: **while** $\lambda_k > 0$ **do**
 - 3: Compute the joining time $\lambda_{k+1}^{\text{join}}$ (11) for $j \in \mathcal{A}_k^c$.
 - 4: Compute the crossing time $\lambda_{k+1}^{\text{cross}}$ (12) for $j \in \mathcal{A}_k$.
 - 5: Compute λ_{k+1} according to (13) and
 - i) if join happens, i.e., $\lambda_{k+1} = \lambda_{k+1}^{\text{join}}$, add the joining index j to \mathcal{A}_k and its sign to s_k ;
 - ii) if cross happens, i.e., $\lambda_{k+1} = \lambda_{k+1}^{\text{cross}}$, remove the crossing index j from \mathcal{A}_k and its sign from s_k .
 - 6: $k = k + 1$.
 - 7: Update $Q_{\mathcal{A}_k}$ according to \mathcal{A}_k and \mathcal{A}_k^c .
 - 8: Compute $a^{(k)}$ and $b^{(k)}$ according to (10).
 - 9: Set $\beta_{\mathcal{A}_k} = a^{(k)} - \lambda_k b^{(k)}$ and $\beta_{\mathcal{A}_k^c} = 0$.
 - 10: **end while**
-

4.3 Numerical example

We consider Nicholson’s graph [15, p. 6] and seek the shortest path between vertex v_1 and v_9 . The iterations of the LARS algorithm (with breakpoints $\lambda_0 = +\infty$, $\lambda_1 = 1/2$, $\lambda_2 = 1/3$, $\lambda_3 = 1/5$, $\lambda_4 = 0.1489$) are depicted in Fig. 1a. It is observed that, at each iteration, edges highlighted in the same color as the corresponding λ are added to the active set and are never removed prior to the last step $\lambda_5 = 0$, as we prove later on in Lemma 6. The algorithm terminates after four iterations when $\lambda_5 = 0$ and a path between vertex v_1 and v_9 is formed. The element-wise path of the lasso solution $\beta(\lambda)$ as λ decreases, is drawn in Fig. 1b.



(a) Nicholson's graph: Edges are added according to breakpoints λ in the same color as in Fig. 1b.



(b) Entries $(\beta(\lambda))(i)$ (corresponding to edges) drawn as functions of λ . Values of λ , where the active edge-set changes, are marked with dashed vertical lines.

Figure 1: The LARS algorithm successively identifies a set of active edges while reducing the tuning/control parameter λ . A vector $\beta(\lambda)$ with information of the length-contribution of the active edge-set is also successively being updated.

Example 1 highlights the correlation between the LARS algorithm and Dijkstra's algorithm. Specifically, the LARS algorithm builds two shortest-path trees, with roots at vertices v_1 and v_9 . This echoes the steps in the bi-directional Dijkstra algorithm discussed in Section 2.2. In Theorem 8, we highlight similarities between the LARS and Dijkstra's algorithms.

5 Relationship between lasso and Dijkstra

Both the LARS as well as the bi-directional Dijkstra algorithm iteratively construct shortest-path trees with roots at v_s and v_t , and terminate when the two trees meet. We prove our main result below by induction. The induction hypothesis is specified next.

Assumption 3 (Induction hypothesis). *At $(k-1)$ th iteration of LARS, the edges in the active set $\mathcal{A}_{k-1} = \mathcal{A}_{k-1}^{(s)} \cup \mathcal{A}_{k-1}^{(t)}$, where $\mathcal{A}_{k-1}^{(s)}$ and $\mathcal{A}_{k-1}^{(t)}$ are disjoint subsets of edges forming trees on vertices $T_{k-1}^{(s)}, T_{k-1}^{(t)} \subset \mathcal{V}$, rooted at v_s and v_t , respectively. The two trees are the shortest-path trees from the roots. Moreover, crossing does not occur at this iteration, i.e., no edges are removed from the active set.*

Our induction starts with the *base case* $k = 1$, where the active set is empty and both trees consist of a single root vertex, $T_0^{(s)} = \{s\}$ and $T_0^{(t)} = \{t\}$. The crossing does not occur since the active set is empty. The proof is based on the following two propositions that provide simplified expressions for the joining and crossing times, derived from Lemma 1 and Assumption 3 that the graph is a tree. The proofs are given in Appendices A and B. Throughout this section and throughout the Appendices, we use D , D^+ , Q , and Q^+ to mean $D_{\mathcal{A}_k}$, $D_{\mathcal{A}_k}^+$, $Q_{\mathcal{A}_k}$, and $Q_{\mathcal{A}_k}^+$ on the active edge set \mathcal{A}_k of the current trees $T_k^{(s)}$ and $T_k^{(t)}$, with $Q := DW^{-1}$. Since each active component is a tree, the incidence has full column rank. Hence, for any tree T , we have $(D_T W_T^{-1})^+ = W_T D_T^+$, where W_T is diagonal with positive entries.

5.1 Joining and crossing times

Proposition 3 (Joining time). *For the edge $e_j = (v_1, v_2)$ where $e_j \in \mathcal{A}_k^c$, the element-wise joining time is*

$$t_{j,k}^{join} = \begin{cases} 0 & \text{if } (v_1, v_2) \in \Omega_k^2 \cup T_k^{(s)2} \cup T_k^{(t)2} \\ \left(|T_k^{(s)}| l_{v_2}^{(s)} - \sum_{v \in T_k^{(s)}} l_v^{(s)} \right)^{-1} & \text{if } (v_1, v_2) \in T_k^{(s)} \times \Omega_k \\ \left(|T_k^{(t)}| l_{v_2}^{(t)} - \sum_{v \in T_k^{(t)}} l_v^{(t)} \right)^{-1} & \text{if } (v_1, v_2) \in T_k^{(t)} \times \Omega_k \\ \left(|T_k^{(s)}| + |T_k^{(t)}| \right) / \Delta & \text{if } (v_1, v_2) \in T_k^{(s)} \times T_k^{(t)} \end{cases}$$

where $\Omega_k = \mathcal{V} \setminus (T_k^{(s)} \cup T_k^{(t)})$, $l_v^{(s)}$ and $l_v^{(t)}$ denote the distance of vertex v to the root s and t respectively, and

$$\Delta := |T_k^{(s)}| |T_k^{(t)}| l_t^{(s)} - |T_k^{(t)}| \sum_{v \in T_k^{(s)}} l_v^{(s)} - |T_k^{(s)}| \sum_{v \in T_k^{(t)}} l_v^{(t)}.$$

Proposition 4 (Crossing time). *For an edge $e_j = (v_1, v_2)$ where $e_j \in \mathcal{A}_k$, the expression $a_j^{(k)} / b_j^{(k)}$ that appears in the definition of crossing time (12) is*

$$\frac{a_j^{(k)}}{b_j^{(k)}} = \begin{cases} \left((|T_k^{(s)}| / |R_j^{(s)}|) \sum_{v \in R_j^{(s)}} l_v^{(s)} - \sum_{v \in T_k^{(s)}} l_v^{(s)} \right)^{-1}, & \text{if } (v_1, v_2) \in T_k^{(s)2} \\ \left((|T_k^{(t)}| / |R_j^{(t)}|) \sum_{v \in R_j^{(t)}} l_v^{(t)} - \sum_{v \in T_k^{(t)}} l_v^{(t)} \right)^{-1}, & \text{if } (v_1, v_2) \in T_k^{(t)2} \end{cases}$$

where $R_j^{(s)}$ and $R_j^{(t)}$ are the subsets of vertices in the tree $T_k^{(s)}$ and $T_k^{(t)}$ respectively, whose path to the root contains the edge e_j .

5.2 Main result

Assuming the induction hypothesis in Assumption 3 holds, we show that the hypothesis also holds at iteration k through the following lemmas.

Lemma 5 (Edge adding). *At iteration k , either the edge connecting $v_{\min}^{(s)}$ to tree $T_k^{(s)}$, or the edge $v_{\min}^{(t)}$ to tree $T_k^{(t)}$ will be added to the active set, where $v_{\min}^{(s)}$ and $v_{\min}^{(t)}$ are vertices with minimum distance to roots v_s and v_t among all other vertices outside the two trees, respectively.*

Proof. First, assume no edge connects the two trees, i.e., the last case of joining time does not happen (the case when it does is studied in Lemma 7). The joining time $\lambda_{j,k}^{\text{join}}$ now reads

$$\max \left\{ \left(|T_k^{(s)}| l_{v_{\min}^{(s)}} - \sum_{v \in T_k^{(s)}} l_v^{(s)} \right)^{-1}, \left(|T_k^{(t)}| l_{v_{\min}^{(t)}} - \sum_{v \in T_k^{(t)}} l_v^{(t)} \right)^{-1} \right\},$$

where the first expression is achieved by the edge that connects $v_{\min}^{(s)}$ to tree $T_k^{(s)}$ and the second is achieved by the edge that connects $v_{\min}^{(t)}$ to tree $T_k^{(t)}$. Hence, one of these two edges is joined to the active set, if crossing does not occur. \square

Remark 2 (No cycles). *Cycles may be created in the following two scenarios: (i) An edge that connects two vertices of a tree is joined; (ii) Two edges that connect the tree to a single vertex, say v , are joined simultaneously. Scenario (i) can not happen because $t_j^{\text{join}} = 0$ for such edges (first case of joining time). Scenario (ii) can not happen, because in order for two edges to join simultaneously, we must have two distinct shortest paths from v to the root, which is not possible according to Assumption 1.*

Lemma 6 (No edge removed). *At iteration k and if $\lambda > 0$, crossing does not take place.*

Proof. To prove that crossing does not take place before the algorithm terminates, we show that $a_j^{(k)}/b_j^{(k)} \geq \lambda_{k-1}$ and hence $a_j^{(k)}/b_j^{(k)} \geq \lambda_k$ for all e_j in the active set, so that crossing time is zero according to its definition (12).

First, we obtain an expression for λ_k and then compare it to crossing times. The value λ_k is determined by the maximum of joining time and crossing time at $(k-1)$ th iteration according to (13). Under Assumption 3, the breakpoint λ_k is the maximum joining time, which takes two possible values, corresponding to the edge that connects to either tree $T_{k-1}^{(s)}$ or tree $T_{k-1}^{(t)}$ as proved in Lemma 5.

Without loss of generality, we now assume the joining happens to the tree $T_{k-1}^{(s)}$. Then,

$$\lambda_{k-1} = \left(|T_{k-1}^{(s)}| l_{v_{\min}^{(s)}} - \sum_{v \in T_{k-1}^{(s)}} l_v^{(s)} \right)^{-1}. \quad (14)$$

Next, we show $a_j^{(k)}/b_j^{(k)} \geq \lambda_{k-1}$ for all e_j that belong to the tree $T_k^{(s)}$. From Proposition 4, we can write $(a_j^{(k)}/b_j^{(k)})$ as

$$\begin{aligned} \frac{a_j^{(k)}}{b_j^{(k)}} &= \left(\frac{1 + |T_{k-1}^{(s)}|}{|R_j^{(s)}|} \sum_{v \in R_j^{(s)}} l_v^{(s)} - l_{v_{\min}^{(s)}} - \sum_{v \in T_{k-1}^{(s)}} l_v^{(s)} \right)^{-1} \\ &\geq \left(|T_{k-1}^{(s)}| l_{v_{\min}^{(s)}} - \sum_{v \in T_{k-1}^{(s)}} l_v^{(s)} \right)^{-1}, \end{aligned}$$

where we used

$$|T_k^{(s)}| = |T_{k-1}^{(s)}| + 1, \quad \sum_{v \in T_k^{(s)}} l_v^{(s)} = l_{v_{\min}^{(s)}} + \sum_{v \in T_{k-1}^{(s)}} l_v^{(s)}, \quad \text{and} \quad l_{v_{\min}^{(s)}} \geq l_v$$

for all $v \in T_k^{(s)}$. The inequality above holds because $v_{\min}^{(s)}$ is the latest vertex that is added to the tree, and other vertices that have already been added have a shorter distance to the root.

The proof of $a_j^{(k)}/b_j^{(k)} \geq \lambda_{k-1}$ for all e_j that belong to the other tree $T_k^{(t)}$ is conceptually similar. One needs to compare $a_j^{(k)}/b_j^{(k)}$ with the joining time of the last edge that has been added to the tree $T_k^{(t)}$ at a certain past iteration, say $k' < k$, and use the fact that $\lambda_k < \lambda_{k'}$. The details are omitted on account of space. \square

Recall from Section 4.2, that the LARS path yields a strictly decreasing sequence of breakpoints $\lambda_0 > \lambda_1 > \dots > \lambda_K = 0$. Hence, once the two trees connect at iteration k , it suffices to verify that all remaining candidate joining and crossing times are zero, which forces $\lambda_{k+1} = 0$.

Lemma 7 (Termination criteria). *The LARS algorithm terminates when the two trees connect.*

Proof. Assume the two trees $T_k^{(s)}$ and $T_k^{(t)}$ become connected at iteration k . This happens when the last expression of joining achieves the maximum joining time, hence $\lambda_k = (|T_k^{(s)}| + |T_k^{(t)}|)/\Delta$, as depicted in Fig. 2. The objective is to show that the algorithm terminates after this, i.e. $\lambda_{k+1} = 0$. We show this by proving that the joining time and crossing time are both zero.

The derivation of element-wise joining time in Proposition 3 reveals that $t_{j,k+1}^{join} = 0$, $\forall e_j \in \mathcal{A}_{k+1}^c$. For the crossing time, the derivation of Proposition 4 yields that for all $e_j \in \mathcal{A}_{k+1}$,

$$\frac{a_j^{(k+1)}}{b_j^{(k+1)}} = \begin{cases} 0, & \text{if } e_j \notin p_{s,t} \\ \left(\sum_{v \in R_j} l_v^{(s)} - \frac{|R_j|}{|T_k^{(t)}| + |T_k^{(s)}|} \sum_{v \in T_k^{(s)} \cup T_k^{(t)}} l_v^{(s)} \right)^{-1}, & \text{otherwise} \end{cases}$$

where $p_{s,t} \subset \mathcal{A}_{k+1}$ is the path from v_s to v_t . Therefore, it remains to show that the crossing time for the edges in $\mathcal{A}_{k+1} \cap p_{s,t}$ are zero. We show this by proving $a_j^{(k+1)}/b_j^{(k+1)} \geq \lambda_k$ for all edges $e_j \in \mathcal{A}_{k+1} \cap p_{s,t}$. Considering the edges that belong to the tree $\mathcal{A}_k^{(s)}$, we have

$$\frac{|T_k^{(s)}| + |T_k^{(t)}|}{\left(a_j^{(k+1)}/b_j^{(k+1)} \right)} = \Delta + |T_k^{(s)}| \sum_{v \in R_j^{(s)}} l_v^{(s)} - |R_j^{(s)}| \sum_{v \in T_k^{(s)}} l_v^{(s)} - |T_k^{(t)}| \sum_{v \in R_j^{(s)}} l_v^{(t)} + |R_j^{(s)}| \sum_{v \in T_k^{(t)}} l_v^{(t)},$$

where $R_j^{(s)}$ are the vertices in the tree $T_k^{(s)}$ such that their path to the root v_s contains e_j . Because $l_v^{(s)} \leq l_{v_2}^{(s)}$ and $l_v^{(t)} \geq l_{v_2}^{(t)}$ for all $v \in R_j^{(s)}$, we have the inequality

$$\frac{|T_k^{(s)}| + |T_k^{(t)}|}{\left(a_j^{(k+1)}/b_j^{(k+1)} \right)} - \Delta \leq |R_j| \left(|T_k^{(s)}| l_{v_2}^{(s)} - \sum_{v \in T_k^{(s)}} l_v^{(s)} - |T_k^{(t)}| l_{v_2}^{(t)} + \sum_{v \in T_k^{(t)}} l_v^{(t)} \right).$$

We claim that the expression in parentheses is negative

$$|T_k^{(s)}|l_{v_2}^{(s)} - \sum_{v \in T_k^{(s)}} l_v^{(s)} - |T_k^{(t)}|l_{v_2}^{(t)} + \sum_{v \in T_k^{(t)}} l_v^{(t)} \leq 0, \quad (15)$$

and if the claim is true, we have

$$a_j^{(k+1)}/b_j^{(k+1)} \geq \left(|T_k^{(s)}| + |T_k^{(t)}| \right) / \Delta = \lambda_k,$$

so that the crossing time is zero for edges $e_j \in \mathcal{A}_k^{(s)}$.

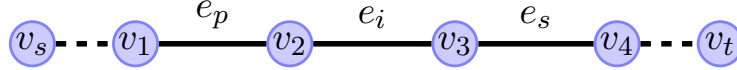


Figure 2: Path $\mathcal{P}_{s,t}$

Finally, we show the claim (15) is true by considering the two possible orders of edge-adding:

i) The edges are added in the order $e_s \rightarrow e_p \rightarrow e_i$, the joining time for e_p and e_i are:

$$\begin{cases} t_{p,k-1}^{\text{join}} &= \left(|T_k^{(s)}|l_{v_2}^{(s)} - \sum_{v \in T_k^{(s)}} l_v^{(s)} \right)^{-1}, \\ t_{i,k-1}^{\text{join}} &= \left(|T_k^{(t)}|l_{v_2}^{(t)} - \sum_{v \in T_k^{(t)}} l_v^{(t)} \right)^{-1}. \end{cases}$$

The assumption that e_p is added before e_i implies $t_{p,k-1}^{\text{join}} > t_{i,k-1}^{\text{join}}$ concluding the claim (15).

ii) The edges are added in the order $e_p \rightarrow e_s \rightarrow e_i$, the joining time for e_p and e_s are:

$$\begin{cases} t_{p,k-2}^{\text{join}} &= \left(|T_k^{(s)}|l_{v_2}^{(s)} - \sum_{v \in T_k^{(s)}} l_v^{(s)} \right)^{-1}, \\ t_{s,k-2}^{\text{join}} &= \left(|T_k^{(t)}|l_{v_2}^{(t)} - \sum_{v \in T_k^{(t)}} l_v^{(t)} \right)^{-1}. \end{cases}$$

The order e_p is added before e_s concludes the claim (15) because $t_{p,k-1}^{\text{join}} > t_{s,k-1}^{\text{join}}$.

The proof that the crossing times for the edges that belong to the tree $\mathcal{A}_k^{(t)}$ is by symmetry and interchanging s and t . \square

We now establish a parallel between the LARS algorithm and the bi-directional Dijkstra algorithm, in that they share the defining feature, terminating when two trees built from opposite directions meet.

Theorem 8 (Equivalence). *The LARS algorithm iteratively builds two shortest-path trees, starting from roots v_s and v_t , and terminates when these two trees connect.*

Proof. Assuming the induction hypothesis in Assumption 3 holds true, we have shown that in the k th iteration: i) edges connecting to vertices with the shortest distance to v_s and v_t are added to the active set (Lemma 5); ii) crossing, where edges are removed from the active set, does not occur when $\lambda > 0$ (Lemma 6). Finally, iii) the algorithm terminates when the two shortest-path trees connect and $\lambda = 0$ (Lemma 7). \square

6 Proximal algorithm for large-scale graph

The LARS algorithm may provide a computational advantage if the desired path only contains a few edges. For large graphs, the number of breakpoints (proportional to the number of edges in the active set), tends to be very large, rendering $\beta(\lambda)$ intractable. The ADMM algorithm, on the other hand, is particularly well-suited for solving large-scale convex optimization problems in a distributed manner due to its scalability [5, 7, 26].

6.1 ADMM and InADMM algorithm

Application of the ADMM to the lasso, as presented in [5, Section 6.4], is based on the reformulation of the lasso problem (4) as follows:

$$\min_{\beta, \alpha \in \mathbb{R}^m} \frac{1}{2} \|y - Q\beta\|_2^2 + \lambda \|\alpha\|_1 + \frac{\rho}{2} \|\beta - \alpha\|_2^2, \text{ s.t. } \alpha = \beta, \quad (16)$$

where $\alpha \in \mathbb{R}^m$ is an additional optimization variable, and ρ is a positive constant.

The *Lagrangian* $L_\rho(\beta, \alpha, u)$ corresponding to the constrained optimization problem (16) is

$$L_\rho = \frac{1}{2} \|y - Q\beta\|_2^2 + \lambda \|\alpha\|_1 + u^T (\beta - \alpha) + \frac{\rho}{2} \|\beta - \alpha\|_2^2,$$

where $u \in \mathbb{R}^m$ is the *Lagrange multiplier*. Let $v \triangleq u/\rho$, the ADMM algorithm consists of the α , β -minimization steps and the step updating the dual variable v . Specifically, the optimal variables β, α, v is computed as

$$\begin{aligned} \beta^k &:= \arg \min_{\beta} L_\rho(\beta, \alpha^{k-1}, v^{k-1}) \\ &= (Q^T Q + \rho I)^{-1} \left(Q^T y + \rho(\alpha^{k-1} - v^{k-1}) \right) \\ \alpha^k &:= \arg \min_{\alpha} L_\rho(\beta^k, \alpha, v^{k-1}) = S_{\lambda/\rho} \left(\beta^k + \frac{1}{\rho} v^{k-1} \right) \\ v^k &:= v^{k-1} + \rho(\beta^k - \alpha^k), \end{aligned} \quad (17)$$

in the $(k-1)$ th iteration. The β -update can be found in [5, Section 4.2] and $S_{\lambda/\rho}$ is the element-wise interpreted proximity operator of the ℓ_1 norm, known as the *soft-thresholding* operator in [5, Section 4.4.3].

To reduce the size and complexity of ADMM, we replace the matrix inversion $(Q^T Q + \rho I)^{-1}$ by

$$(Q^T Q + \rho I)^{-1} = \frac{1}{\rho} \left(I - Q^T (Q Q^T + \rho I)^{-1} Q \right), \quad (18)$$

using the *matrix identity*, which instead involves $(Q^T Q + \rho I)^{-1}$. We will show this step significantly reduces the complexity of the algorithm in the next section. To further reduce the complexity of

ADMM for large-scale graphs, we use the InADMM algorithm introduced in [26] whose key idea is to approximately solve a system of linear equations instead of evaluating the matrix inversion exactly, using the matrix identity (18) to replace the β update in (17) with

$$\begin{aligned} h^{k-1} &:= Q^T y + \rho(\alpha^{k-1} - v^{k-1}) \\ \eta^k &:= (QQ^T + \rho I)^{-1} Q h^{k-1}, \\ \beta^k &:= \frac{1}{\rho}(h^{k-1} - Q^T \eta^k) \end{aligned}$$

and computes η^k approximately using the *conjugate gradient* (CG) method [13].

Remark 3 (Stopping criteria). *Both ADMM and InADMM use the standard primal-dual residual test. With $r_k = \beta_k - \alpha_k$ and $s_k = \alpha_k - \alpha_{k-1}$, a stopping criterion is when $\|r_k\|_2 \leq \varepsilon_{\text{abs}}\sqrt{m} + \varepsilon_{\text{rel}} \max\{\|\beta_k\|_2, \|\alpha_k\|_2\}$, or when $\|s_k\|_2 \leq \varepsilon_{\text{abs}}\sqrt{m} + \varepsilon_{\text{rel}}\|v_k\|_2$. We use $(\varepsilon_{\text{abs}}, \varepsilon_{\text{rel}}) = (10^{-8}, 10^{-6})$, with m the number of edges. In InADMM, the inner CG solver uses relative residual 10^{-8} (up to 2×10^3 iterations).*

6.2 Warm-start, Parallel lasso, and complexity

The lasso formulation and the ADMM solvers admit remark features that can not be found in A* search algorithm. We postulate two key features that are brought into the shortest path problem.

Firstly, distinguished from Dijkstra's algorithm, the ADMM allows the input of any initializer (potential-path), that may be used in tracking the graph topological changes. The problem then becomes correcting/updating the shortest path with an initial guess/prior as inputs. Our approach shows a fast convergence under such circumstances, see Fig. 4.

Notably, the problem can be generalized through *parallel lasso*, addressing the multi-pair/all-pair shortest path problem defined as:

$$\arg \min_{\beta \in \mathbb{R}^m} \left\{ \sum_{i=1, \dots, N} \frac{1}{2} \|\mathbf{y}_i - Q\beta_{(i)}\|_2^2 + \lambda \|\beta_{(i)}\|_1 \right\} \quad (19)$$

where the i -th column of \mathbf{y} is the indicator vector of path, and thus we defined $\mathbf{y}_{1, \dots, N} = [y_{(1)}, \dots, y_{(N)}]$ and $\beta = [\beta_{(1)}, \dots, \beta_{(N)}]$. The framework (17) is thus solves a multi-pair shortest path problem. The optimal variables in ADMM can be easily extended vector-wise while the dominated matrix inverse only needs to be computed once for all. Specifically, when \mathbf{y} characterizes all pairs of vertices, Problem (19) becomes the lasso formulation of all-pairs shortest path problem.

We use *worst-case complexity* (denoted as $\mathcal{O}(\cdot)$) to evaluate the algorithms' performance. It quantifies the operations of the algorithm in the worst case, see [7, Appendix C], [9]. The complexity of ADMM is dominated by the matrix inversion $(Q^T Q + \rho I)_{m \times m}^{-1}$, which is of order $\mathcal{O}(m^3)$ (e.g. using *Cholesky decomposition*). However, by utilizing the matrix identity (18), this complexity is reduced to $\mathcal{O}(n^3)$. The most costly step in the CG method is the matrix-vector multiplication $(QQ^T + \rho I)x$ where $x \in \mathbb{R}^n$. This has a complexity of $\mathcal{O}(m)$ because the weighted incidence matrix Q has $2m$ nonzero elements. Assuming the CG algorithm terminates in T_{CG} iterations, the complexity of the CG step in InADMM algorithm is of order $\mathcal{O}(mT_{CG})$. Noticing the complexity of other operations in InADMM is at most $\mathcal{O}(m)$, we summarize the complexities in Table 1 as below.

⁶Per iteration, both methods converge within 40 steps for a graph with 17291 edges, see Fig. 4.

⁷ $T_{CG} \ll n$ and scalable with respect to the size of the graph. Empirically, we have $T_{CG} = 350$ for graph with 4422

Variables	η	$\beta(\text{Cholesky})$	α	v
ADMM ⁶	$\mathcal{O}(nm)$	$\mathcal{O}(n^3)$	$\mathcal{O}(m)$	$\mathcal{O}(m)$
InADMM ⁷	$\mathcal{O}(mT_{CG})$	$\mathcal{O}(m)$	$\mathcal{O}(m)$	$\mathcal{O}(m)$

Table 1: Complexities of ADMM and InADMM per iteration.

6.3 Example 1: Intelligent scissors on image

We first consider “*intelligent scissors*”, an image segmentation technique that is commonly used in computer vision [14]. It creates a *grid graph* over the image with each pixel represented by a vertex, and is connected to its 8 neighboring pixels through edges. The edge weights are assigned by a cost function [14, Section 3] based on image features. The objective is to identify a boundary between the portraits and the background, which turns out to be equivalent to finding the shortest path between selected pixels (marked in green) over the generated graph. The segmentation is obtained by identifying the edges in the shortest path. Herein, we use an image with 4422 pixels. The edges, detected by constructing shortest paths using three different methods and colored in red, are drawn in Fig. 3 (The code used in the paper is available at github.com/dytroshut/Lasso-shortest-path.git; functions in the code can be found in [6]). For the InADMM, we utilized the CG method from [13, 26]. The convergence rates of ADMM, InADMM, and Basis Pursuit⁸ [5, Section 6.1], are shown in Fig. 4. Further, to highlight the efficiency of lasso’s distributed implementation, we used InADMM (with a pre-specified path as input).

6.4 Example 2: Route planning on road networks

Next, we study “*route planning*” on urban road maps, a standard task in transportation. This induces an *undirected road graph* with intersections as vertices and street segments as edges. Edge weights are travel times, computed from segment length and nominal speed, with turn costs at busy junctions. The minimum-time trip between two addresses is then the shortest path on this weighted graph. To highlight contrasting geometries, we use city-scale OpenStreetMap [25] extracts for Athens ($n=1009$, $m=2340$) and Amsterdam ($n=1031$, $m=2037$). The recovered routes, computed by Dijkstra (yellow), ADMM (red), and InADMM (green), are shown in Fig. 5. These graphs are sparse and close to planar, so effective routes rise to arterial and return to local streets near the destination.

We build the signed incidence from the road graph and use travel-time edge weights. The regularization is set to $\lambda = 10^{-4}\lambda_{\max}$, where λ_{\max} is the standard lasso threshold. ADMM uses a penalty $\rho = 1$ and over-relaxation $\alpha = 1.8$ with a sparse Cholesky solver. InADMM keeps the same splitting and replaces the direct solver with a preconditioned conjugate-gradient step on the normal equations (diagonal preconditioner, relative tolerance 10^{-8} , maximum 2000 iterations). To avoid degeneracies and ensure a unique s - t route, we apply a one-time strictly positive perturbation to all edge weights and use the same perturbed weights for Dijkstra, ADMM, and InADMM.

Then, for scalability, we repeat the experiment on the Amsterdam map with finer segmentation at two larger sizes, $n = 4699$, $m = 8270$ and $n = 9379$, $m = 14571$ (see Fig. 6). With the same settings

vertices and $T_{CG} = 320$ for graph with 5694 vertices. To reach ϵ accuracy, using $\mathcal{O}(1/\epsilon)$ iteration complexity [26, Theorem 4.1], we conclude overall $\mathcal{O}(nm/\epsilon)$ and $\mathcal{O}(n^3/\epsilon)$ complexity for update of η in InADMM and β in ADMM, respectively.

⁸Basis Pursuit is a technique to obtain sparse solution to an underdetermined system of linear equations.

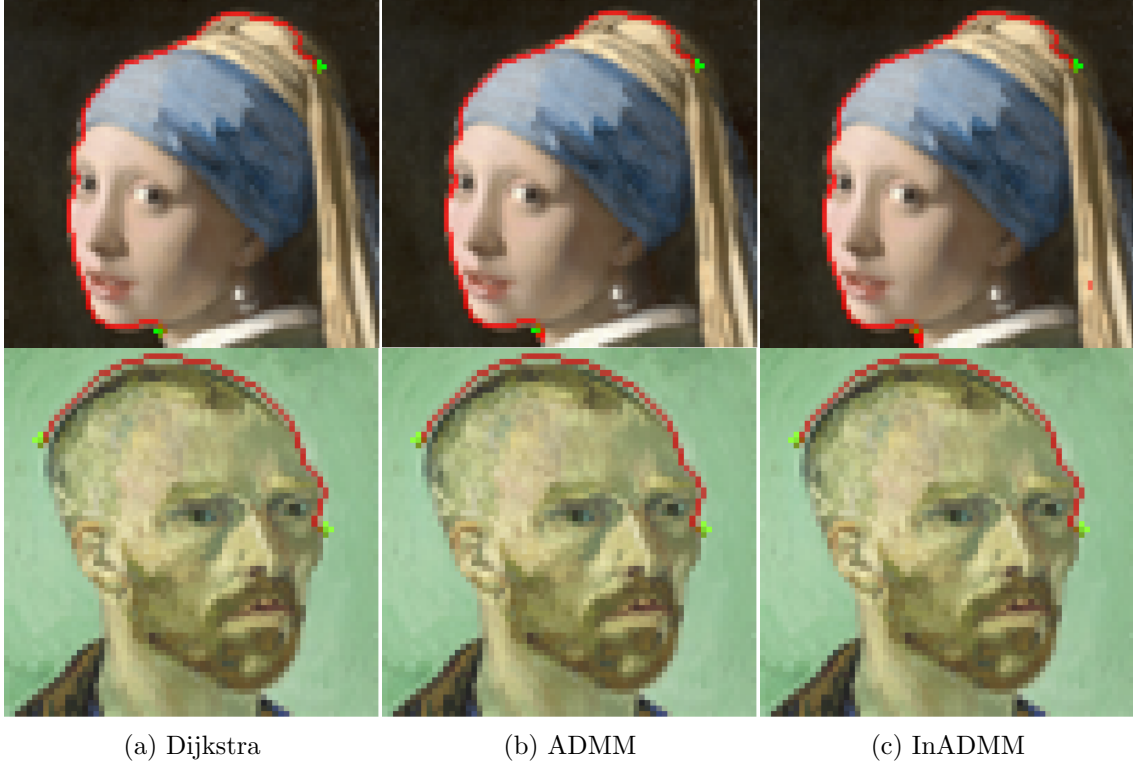


Figure 3: “Edge detection” in an image as a short path, highlighted in red, and obtained using Dijkstra’s algorithm (Fig. 3a), as well as using the lasso solution β in ADMM and InADMM in Fig. 3b and Fig. 3c, respectively.

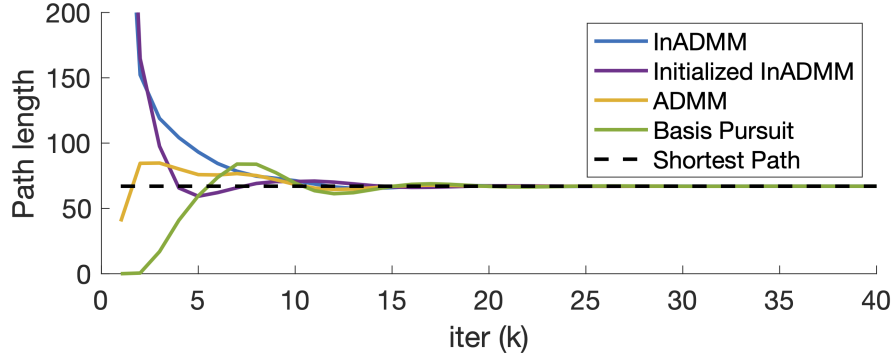


Figure 4: Example based on the image ($n = 4422$ and $m = 17291$): “Edge in image” identified via InADMM, InADMM with initializer, ADMM, and Basis pursuit. These converge in 36, 34, 29, 47 steps, respectively, with running times 1.7308, 1.7618, 4.0249, 35.7527 seconds in MATLAB clock. Also, the running times for solving the linear program (3b) using three methods (*dual-simplex* and *interior-point(-legacy)*) are 26.6145, 29.3866, 32.2845 seconds.

as in Fig. 5 and $\lambda = 10^{-6}\lambda_{\max}$, the InADMM lasso path remains efficient and robust, recovering essentially the same minimum-time corridor on the higher-resolution graphs. A complementary effect appears when we decrease the penalty to $\lambda = 10^{-7}\lambda_{\max}$. The solution begins to place nonzero weights on several nearly equivalent routes, so the highlighted support widens to reflect

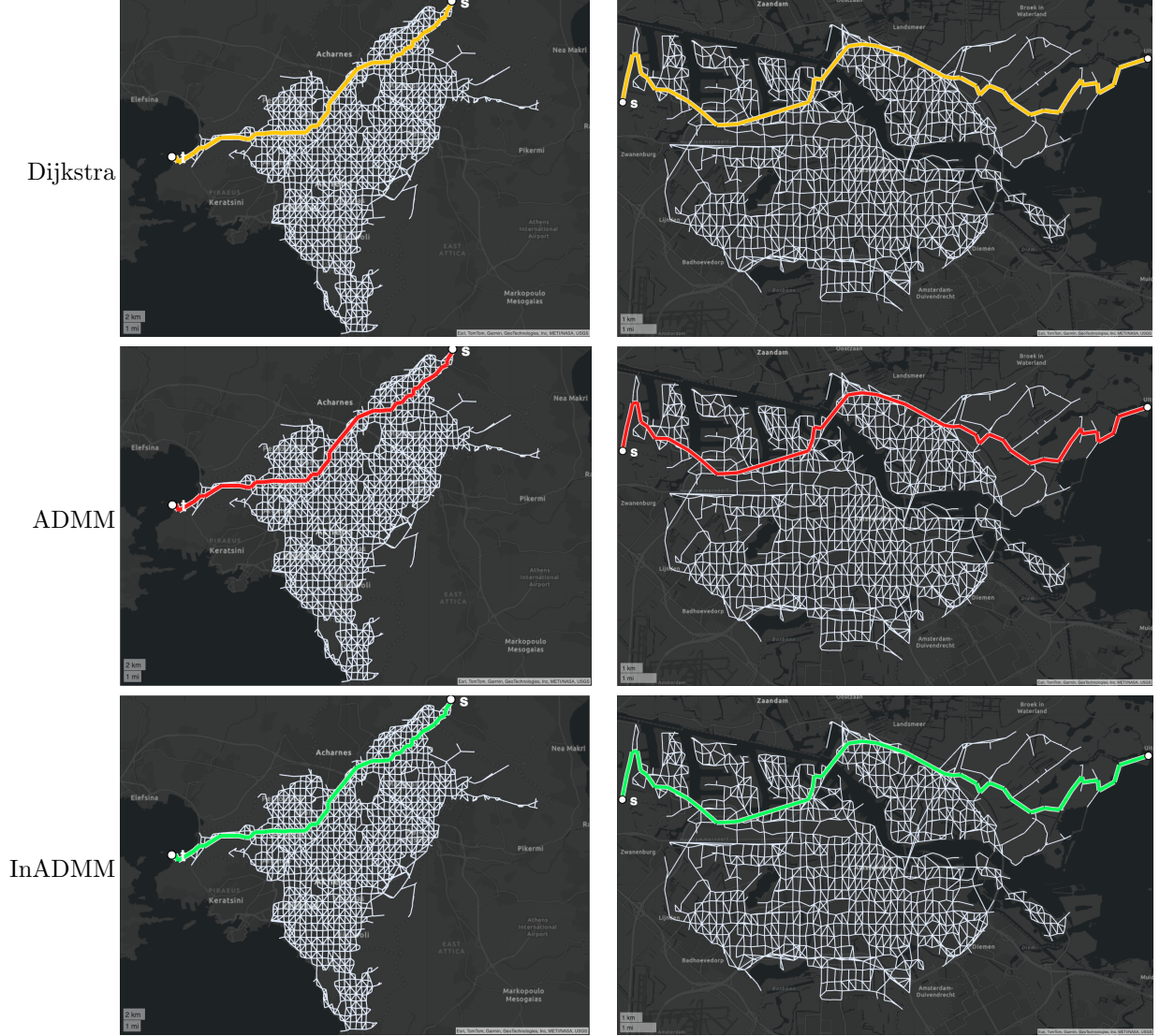
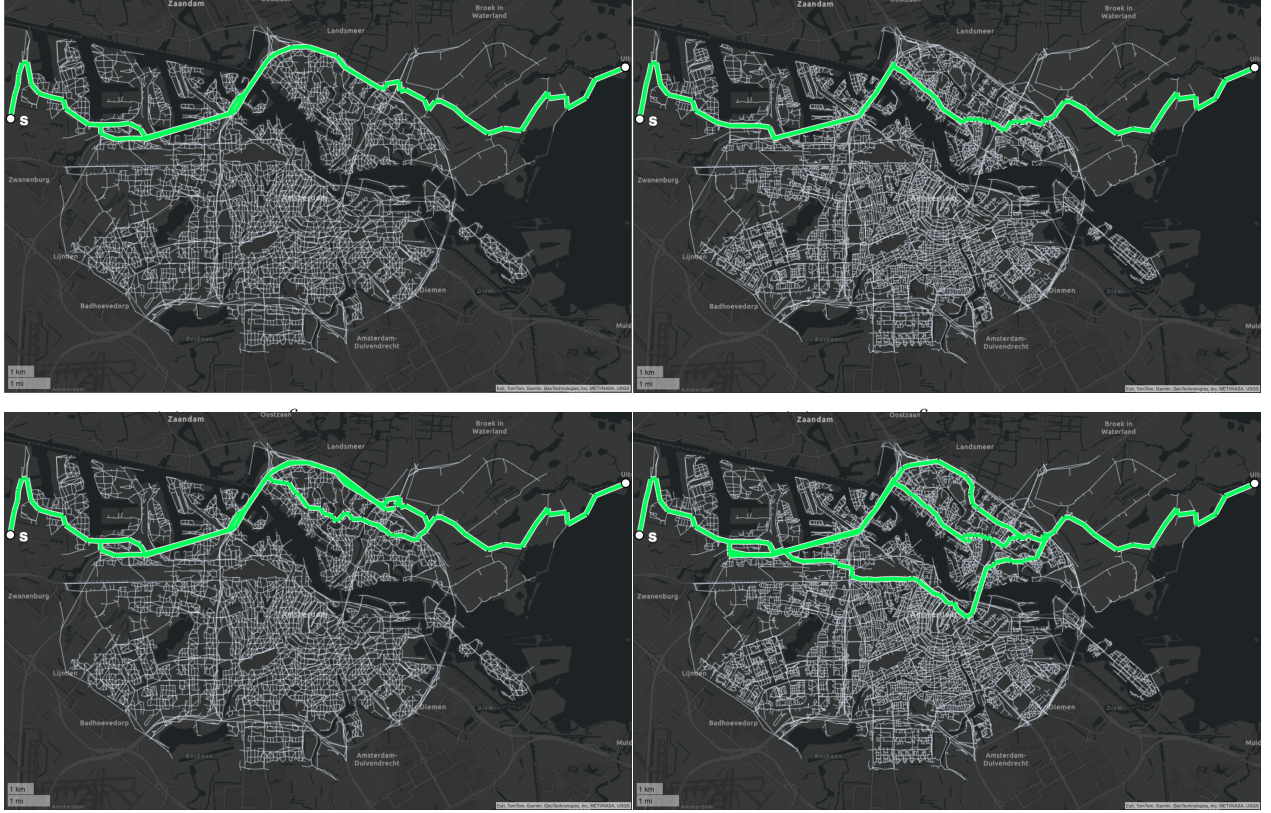


Figure 5: “Minimum-time trip” planning on Athens and Amsterdam road networks. Shortest paths from Dijkstra (yellow) and supports of the lasso solution β recovered by ADMM (red) and InADMM (green) are overlaid.

multiple plausible arterials. The phenomenon is more pronounced at higher resolution, where finer segmentation introduces additional near-equivalences between the same source and destination, as in Fig. 6.

6.5 Example 3: Multi-hop shortest-path routing on random geometric networks

Lastly, we build random geometric graphs for “*multi-hop routing*”. We take the node set from the largest weakly connected component of the CiteSeerX network (IDs only, citation edges ignored) [17], place each node uniformly at random in $[0, 1]^2$, and connect pairs whose Euclidean distance is at most a radius r . We increase r until the giant component contains at least 98% of the nodes, then keep that component ($n = 2997$, $m = 14149$).



(c) $\lambda = 10^{-7}\lambda_{\max}$, $n = 4699$

(d) $\lambda = 10^{-7}\lambda_{\max}$, $n = 9379$

Figure 6: Scalability and robustness on the same Amsterdam road map under finer segmentation. For $n = 4699$, $m = 8270$ and $n = 9379$, $m = 14571$, the InADMM lasso path with $\lambda = 10^{-6}\lambda_{\max}$ recovers essentially the same minimum-time corridor. With $\lambda = 10^{-7}\lambda_{\max}$, the support broadens, reflecting several nearly equivalent alternatives. All runs use identical weight jitter/tie-break and the same source-destination.

Edge costs model transmit effort as squared Euclidean distance ($\alpha = 2$). To avoid degeneracies and ensure a unique s - t route, we apply a one-time strictly positive perturbation to all edge weights and use the same perturbed weights for Dijkstra, ADMM, and InADMM. The source s is the left-most node; the target t is the node with the largest finite weighted distance from s under these weights, which yields a long left-to-right route that threads dense patches and skirts voids. All remaining solver settings (choice of λ , ADMM/InADMM parameters, and stopping criteria) match Example 2. We then repeat the same construction at two larger scales, yielding $(n, m) = (5997, 30918)$ and $(n, m) = (8989, 48819)$. As before, s is chosen as the left-most node and t as the node with the largest finite weighted distance from s . Across both sizes, the recovered lasso support (InADMM) coincides with the Dijkstra shortest path at our display thresholds, no side branches appear, and the route remains unique by construction.

7 Concluding remarks

The main contribution in this work is to point out that short paths in graphs, sought via formulation as a lasso problem, has computational and implementation advantages. Specifically, the use of

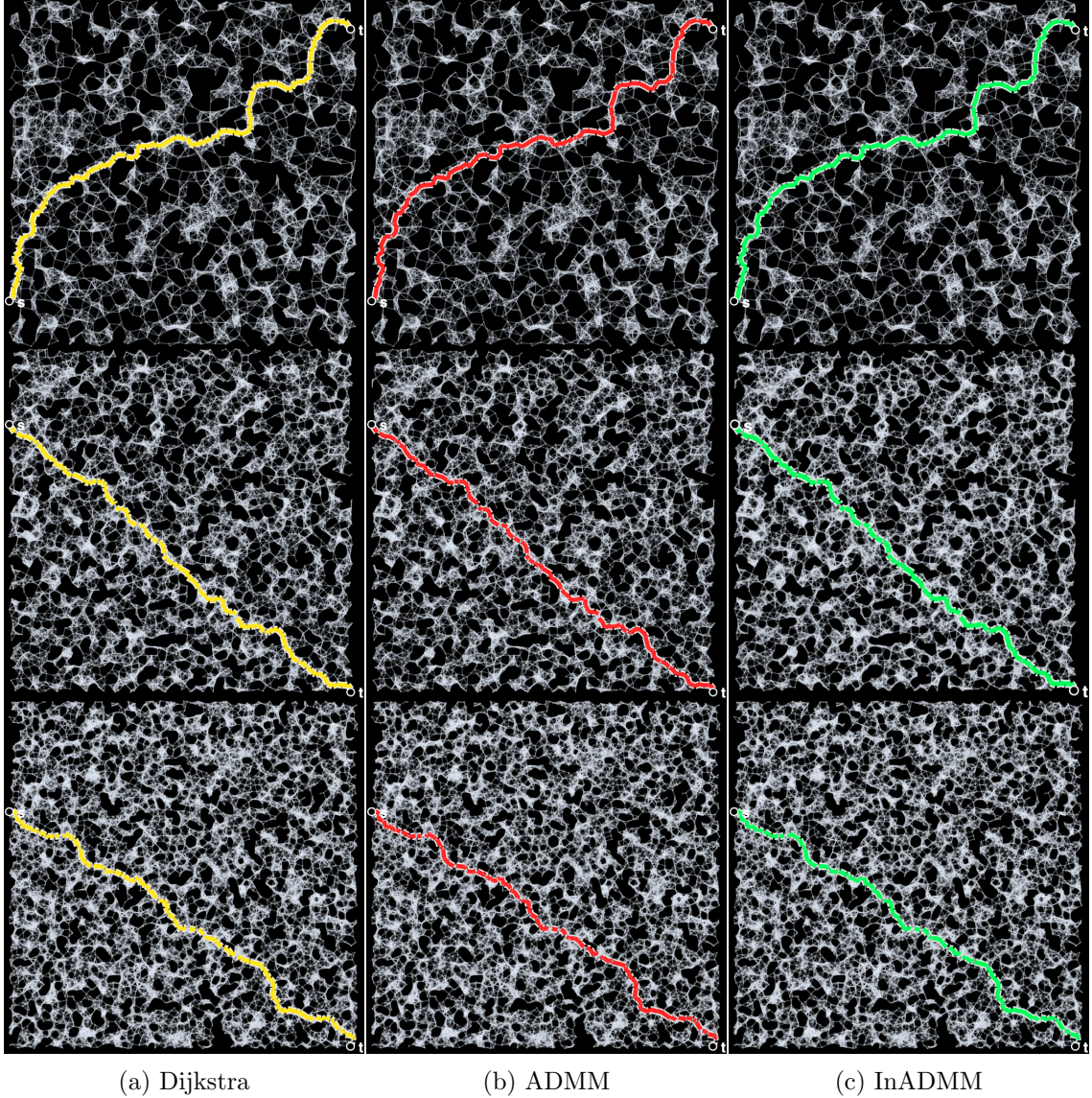


Figure 7: Multi-hop routing on random geometric graphs. Shortest path from Dijkstra (yellow) and supports of the lasso solution β recovered by ADMM (red) and InADMM (green) are overlaid. From top to bottom, graph size increases: top row $(n, m) = (2997, 14149)$, middle row $(5997, 30918)$, bottom row $(8989, 48819)$.

ADMM algorithms for large graphs reduces computational complexity and allows for distributed implementation. Extension of the framework to one that can cope with negative weights is desirable, but at present, not available.

Acknowledgment

This research has been supported in part by the NSF under ECCS-2347357, AFOSR under FA9550-24-1-0278, and ARO under W911NF-22-1-0292.

Appendix

A Proof of Proposition 4

For simplicity, we drop the iteration subscript k in our derivations. $D_{\mathcal{A}}$ is the incidence matrix formed by the edges in the active set. The graph formed by \mathcal{A} consists of two disjoint trees $T^{(s)}$, $T^{(t)}$, and the set of isolated vertices Ω . We decompose the rows of matrix $D_{\mathcal{A}}$ into rows corresponding to these three subsets and express $D_{\mathcal{A}}$ and $D_{\mathcal{A}}^+$ according to

$$D_{\mathcal{A}} = \begin{bmatrix} D_{\mathcal{A}^{(s)}} & \mathbf{0} \\ \mathbf{0} & \mathbf{0} \\ \mathbf{0} & D_{\mathcal{A}^{(t)}} \end{bmatrix},$$

and

$$D_{\mathcal{A}}^+ = \begin{bmatrix} D_{\mathcal{A}^{(s)}}^+ & \mathbf{0} & \mathbf{0} \\ \mathbf{0} & \mathbf{0} & D_{\mathcal{A}^{(t)}}^+ \end{bmatrix},$$

with $D_{\mathcal{A}^{(s)}}$, $D_{\mathcal{A}^{(t)}}$ are the incidence matrix for the tree $T^{(s)}$ and $T^{(t)}$ respectively, and $\mathbf{0}$ represents all-zeros matrices of appropriate dimensions. We use this expression and Lemma 1 to compute a and b by their definition (10)

$$\begin{aligned} a &= (Q_{\mathcal{A}}^T Q_{\mathcal{A}})^+ Q_{\mathcal{A}}^T y = Q_{\mathcal{A}}^+ y = W_{\mathcal{A}} D_{\mathcal{A}}^+ y \\ &= W_{\mathcal{A}} \begin{bmatrix} D_{\mathcal{A}^{(s)}}^+ & \mathbf{0} & \mathbf{0} \\ \mathbf{0} & \mathbf{0} & D_{\mathcal{A}^{(t)}}^+ \end{bmatrix} \begin{bmatrix} 1 \\ \mathbf{0} \\ -1 \end{bmatrix} \\ &= \begin{bmatrix} -\frac{1}{|T^{(s)}|} W_{\mathcal{A}^{(s)}} P^{(s)} \mathbb{1}_{|T^{(s)}|} \\ +\frac{1}{|T^{(t)}|} W_{\mathcal{A}^{(t)}} P^{(t)} \mathbb{1}_{|T^{(t)}|} \end{bmatrix}, \end{aligned}$$

where $P^{(s)}$ and $P^{(t)}$ are the path matrix for tree $T^{(s)}$ and $T^{(t)}$ respectively. Then,

$$\begin{aligned} b &= (Q_{\mathcal{A}}^T Q_{\mathcal{A}})^+ s \\ &= W_{\mathcal{A}} D_{\mathcal{A}}^+ (D_{\mathcal{A}}^T)^+ W_{\mathcal{A}} s \\ &= \begin{bmatrix} -W_{\mathcal{A}^{(s)}} \left(P^{(s)} \mathcal{L}^{(s)} - \frac{1}{|T^{(s)}|} P^{(s)} \mathbb{1}_s \mathbb{1}_s^T \mathcal{L}^{(s)} \right) \\ +W_{\mathcal{A}^{(t)}} \left(P^{(t)} \mathcal{L}^{(t)} - \frac{1}{|T^{(t)}|} P^{(t)} \mathbb{1}_t \mathbb{1}_t^T \mathcal{L}^{(t)} \right) \end{bmatrix}, \end{aligned}$$

where $\mathcal{L}^{(s)} \triangleq -(P^{(s)})^T W_{\mathcal{A}^{(s)}} s$ is a vector of size $|T^{(s)}|$ corresponding to vertices in the tree $T^{(s)}$. The component of $\mathcal{L}^{(s)}$, corresponding to vertex $v \in T^{(s)}$, is equal to $l_v^{(s)}$, i.e. the length of the path from v to the root s . The vector $\mathcal{L}^{(t)} \triangleq (P^{(t)})^T W_{\mathcal{A}^{(t)}} s$ has a similar interpretation, but for vertices of tree $T^{(t)}$ and the difference of the definitions of $\mathcal{L}^{(s)}$ and $\mathcal{L}^{(t)}$ is resulted in the different signs of the two elements in b .

Putting the results for vectors a and b together, the ratio a_j/b_j for $e_j \in \mathcal{A}^{(s)}$ is

$$\frac{a_j}{b_j} = \frac{\frac{1}{|T^{(s)}|} w_j |R_j|}{w_j (\sum_{v \in R_j} l_v^{(s)} - \frac{|R_j|}{|T^{(s)}|} \sum_{v \in T^{(s)}} l_v^{(s)})},$$

where R_j is the set of non-zero components of the j th row of $P^{(s)}$ since the same edge e_j shares the same direction along all the paths in a tree. This concludes our proof for $e_j \in \mathcal{A}^{(s)}$. The derivation for $e_j \in \mathcal{A}^{(t)}$ is similar.

B Proof of Proposition 3

By definition of joining time (11), for all $e_j \in \mathcal{E}$, reads

$$t_j^{\text{join}} = \frac{\frac{1}{w_j} D_j^T (Q_{\mathcal{A}} a - y)}{\frac{1}{w_j} D_j^T (Q_{\mathcal{A}} b) \pm 1} = \frac{D_j^T (Q_{\mathcal{A}} a - y)}{D_j^T (Q_{\mathcal{A}} b) \pm w_j}, \quad (20)$$

with the choice \pm dictated by t_j^{join} taking positive value. We now obtain expressions for the terms in parentheses. First, the term $(Q_{\mathcal{A}} a - y)$ in the numerator equals to

$$\begin{aligned} D_{\mathcal{A}} D_{\mathcal{A}}^+ y - y &= \begin{bmatrix} D_{\mathcal{A}^{(s)}} & \mathbf{0} \\ \mathbf{0} & \mathbf{0} \\ \mathbf{0} & D_{\mathcal{A}^{(t)}} \end{bmatrix} \begin{bmatrix} D_{\mathcal{A}^{(s)}}^+ & \mathbf{0} & \mathbf{0} \\ \mathbf{0} & \mathbf{0} & D_{\mathcal{A}^{(t)}}^+ \end{bmatrix} y - y \\ &= \begin{bmatrix} -\frac{1}{|T^{(s)}|} \mathbb{1}_s \\ \mathbf{0}_{|\Omega|} \\ +\frac{1}{|T^{(t)}|} \mathbb{1}_t \end{bmatrix}, \end{aligned} \quad (21)$$

where we used

$$D D^+ = I - \frac{1}{\mathbb{1}^T \mathbb{1}} \mathbb{1} \mathbb{1}^T$$

for incidence matrices $D_{\mathcal{A}^{(s)}}$ and $D_{\mathcal{A}^{(t)}}$ of the two disjoint trees [3, Lemma 2.15], and $\mathbf{0}_{|\Omega|}$ denotes all-zero (column) vectors of size $|\Omega|$. Second, the term $(Q_{\mathcal{A}} b)$ in the denominator equals to $(D_{\mathcal{A}} D_{\mathcal{A}}^+ (D_{\mathcal{A}}^T)^+ W_{\mathcal{A}} s)$ and moreover, it equals to

$$(D_{\mathcal{A}}^+)^T W_{\mathcal{A}} s = \begin{bmatrix} -\mathcal{L}^{(s)} + \frac{1}{|T^{(s)}|} \mathbb{1}_s \mathbb{1}_s^T \mathcal{L}^{(s)} \\ \mathbf{0}_{|\Omega|} \\ \mathcal{L}^{(t)} - \frac{1}{|T^{(t)}|} \mathbb{1}_t \mathbb{1}_t^T \mathcal{L}^{(t)} \end{bmatrix}. \quad (22)$$

where $\mathcal{L}^{(s)}$ (resp. $\mathcal{L}^{(t)}$) collects the root-to-vertex distances $l_v^{(s)}$ on $T^{(s)}$ (resp. $l_v^{(t)}$ on $T^{(t)}$).

Evaluating the expression in (20) for edge $e_j = (v_1, v_2) \in \mathcal{A}^c$ and without loss of generality, assume the assigned direction is from v_1 to v_2 , the joining time is categorized into three separate cases.

i) If $(v_1, v_2) \in \Omega^2 \cup T^{(s)2} \cup T^{(t)2}$, i.e., the two ends of e_j belongs to or isolated from the trees, we have $t_j^{\text{join}} = 0$ by the numerator (21) and the definition of D_j^T .

ii) If $(v_1, v_2) \in (T^{(s)} \times \Omega) \cup (T^{(t)} \times \Omega)$, Without loss of generality, assume $v_1 \in T^{(s)}$ and $v_2 \in \Omega$, using the blocks above, we have

$$D_j^T (Q_{\mathcal{A}} a - y) = \frac{1}{|T^{(s)}|}, \quad D_j^T (Q_{\mathcal{A}} b) = l_{v_2}^{(s)} - \frac{1}{|T^{(s)}|} \sum_{v \in T^{(s)}} l_v^{(s)}.$$

The joining now reads

$$\begin{aligned} t_j^{\text{join}} &= (|T^{(s)}|l_{v_1}^{(s)} - \mathbb{1}^T \mathcal{L}_v^{(s)} \pm |T^{(s)}|w_j)^{-1} \\ &= \left(|T^{(s)}|(l_{v_1}^{(s)} + w_j) - \mathbb{1}^T \mathcal{L}_v^{(s)}\right)^{-1} \\ &= \left(|T^{(s)}|l_{v_2}^{(s)} - \sum_{v \in T^{(s)}} l_v^{(s)}\right)^{-1}. \end{aligned}$$

(The expression is equivalent to using $l_{v_2}^{(s)} = l_{v_1}^{(s)} + w_j$ upon joining.)

iii) If $(v_1, v_2) \in T^{(s)} \times T^{(t)}$, then

$$D_j^\top(Q_{\mathcal{A}}a - y) = \frac{1}{|T^{(s)}|} + \frac{1}{|T^{(t)}|}, \quad D_j^\top(Q_{\mathcal{A}}b) = \left(l_{v_1}^{(s)} - \overline{l^{(s)}}_{T^{(s)}}\right) + \left(l_{v_2}^{(t)} - \overline{l^{(t)}}_{T^{(t)}}\right),$$

where $\overline{l^{(s)}}_{T^{(s)}} = \frac{1}{|T^{(s)}|} \sum_{v \in T^{(s)}} l_v^{(s)}$ and $\overline{l^{(t)}}_{T^{(t)}} = \frac{1}{|T^{(t)}|} \sum_{v \in T^{(t)}} l_v^{(t)}$. At the connection step, for the edge

that realizes the maximum joining time we have $l_{v_1}^{(s)} + w_j + l_{v_2}^{(t)} = l_t^{(s)}$ (i.e., the s - t distance), hence the denominator in (20) equals

$$l_t^{(s)} - \overline{l^{(s)}}_{T^{(s)}} - \overline{l^{(t)}}_{T^{(t)}} = \frac{\Delta}{|T^{(s)}||T^{(t)}|},$$

with

$$\Delta = |T^{(s)}||T^{(t)}|l_t^{(s)} - |T^{(t)}| \sum_{v \in T^{(s)}} l_v^{(s)} - |T^{(s)}| \sum_{v \in T^{(t)}} l_v^{(t)}.$$

Therefore

$$t_j^{\text{join}} = \frac{\frac{1}{|T^{(s)}|} + \frac{1}{|T^{(t)}|}}{\frac{\Delta}{|T^{(s)}||T^{(t)}|}} = \frac{|T^{(s)}| + |T^{(t)}|}{\Delta}.$$

C Proof of Lemma 2

The proof is based on the sufficient condition for the uniqueness of the lasso solution [21, Lemma 2], which states that “*For any β , Q , and $\lambda > 0$, if $\text{null}(Q_{\mathcal{A}}) = \{0\}$ (or equivalently if $\text{rank}(Q_{\mathcal{A}}) = |\mathcal{A}|$), the lasso solution and the active set \mathcal{A} are always unique.*” Thus, we prove the lasso solution $\beta(\lambda)$ is unique for every $\lambda > 0$ by showing that $\text{rank}(Q_{\mathcal{A}}) = |\mathcal{A}|$ is true for every $Q_{\mathcal{A}}$.

In Section 5, we showed that the active set forms two disjoint trees (Lemma 5 and 6). Hence,

$$Q_{\mathcal{A}} = [Q_{\mathcal{A}^{(s)}}, \quad Q_{\mathcal{A}^{(t)}}] = \begin{bmatrix} D_{\mathcal{A}^{(s)}} W_{\mathcal{A}^{(s)}}^{-1}, & D_{\mathcal{A}^{(t)}} W_{\mathcal{A}^{(t)}}^{-1} \end{bmatrix},$$

with $D_{\mathcal{A}_k^{(t)}}$ and $D_{\mathcal{A}_k^{(s)}}$ are incidence matrices of two trees positively weighted by the weighted matrices $W_{\mathcal{A}_k^{(s),(t)}}$. The null space (*kernel*) of the incidence matrix of a tree is empty because there is no cycle in the tree by its definition, so the rank of its incidence matrix is equal to the number of columns, i.e., the rank of $Q_{\mathcal{A}}$ is equal to $|\mathcal{A}|$. Therefore, the sufficient condition for the unique lasso solution is satisfied.

References

- [1] Ravindra K. Ahuja, Thomas L. Magnanti, and James B. Orlin. *Network flows. Theory, Algorithms, and Applications*. Prentice Hall, 1988.
- [2] Ravindra K. Ahuja, Kurt Mehlhorn, James Orlin, and Robert E. Tarjan. Faster algorithms for the shortest path problem. *Journal of the ACM*, 37(2):213–223, 1990.
- [3] Ravindra B. Bapat. *Graphs and matrices*, volume 27. Springer, 2010.
- [4] Hannah Bast, Daniel Delling, Andrew Goldberg, Matthias Müller-Hannemann, Thomas Pajor, Peter Sanders, Dorothea Wagner, and Renato F. Werneck. Route planning in transportation networks. In *Algorithm engineering*, pages 19–80. Springer, 2016.
- [5] Stephen Boyd, Neal Parikh, Eric Chu, Borja Peleato, and Jonathan Eckstein. Distributed optimization and statistical learning via the alternating direction method of multipliers. *Foundations and Trends in Machine learning*, 3(1):1–122, 2011.
- [6] Stephen Boyd, Neal Parikh, Eric Chu, Borja Peleato, and Jonathan Eckstein. Matlab scripts for alternating direction method of multipliers, 2011.
- [7] Stephen Boyd and Lieven Vandenbergh. *Convex optimization*. Cambridge university press, 2004.
- [8] Srinivasan Chandrasekar and Pradip K. Srimani. A self-stabilizing distributed algorithm for all-pairs shortest path problem. *Parallel Algorithms and Applications*, 4(1-2):125–137, 1994.
- [9] Thomas H. Cormen, Charles E. Leiserson, Ronald L. Rivest, and Clifford Stein. *Introduction to algorithms*. MIT press, 2022.
- [10] Edsger W. Dijkstra. A note on two problems in connexion with graphs. *Numerische mathematik*, 1(1):269–271, 1959.
- [11] Anqi Dong, Amirhossein Taghvaei, and Tryphon T. Georgiou. Lasso formulation of the shortest path problem. In *2020 59th IEEE Conference on Decision and Control (CDC)*, pages 402–407. IEEE, 2020.
- [12] Michael L. Fredman and Robert Endre Tarjan. Fibonacci heaps and their uses in improved network optimization algorithms. *Journal of the ACM*, 34(3):596–615, 1987.
- [13] Magnus R. Hestenes and Eduard Stiefel. Methods of conjugate gradients for solving linear systems. *Journal of Research of the National Bureau of Standards*, 49(6):409–436, 1952.
- [14] Eric N. Mortensen and William A. Barrett. Intelligent scissors for image composition. In *Proceedings of the 22nd annual conference on Computer graphics and interactive techniques*, pages 191–198, 1995.
- [15] Ira Pohl. Bidirectional and heuristic search in path problems. Technical report, Technical Report SLAC-104, Stanford Linear Accelerator Center, Stanford, California, 1969.
- [16] Michalis Potamias, Francesco Bonchi, Carlos Castillo, and Aristides Gionis. Fast shortest path distance estimation in large networks. In *Proceedings of the 18th ACM conference on Information and knowledge management*, 2009.
- [17] Ryan A. Rossi and Nesreen K. Ahmed. The network data repository with interactive graph analytics and visualization. In *AAAI*, 2015.

- [18] Moshe Sniedovich. Dijkstra’s algorithm revisited: the dynamic programming connexion. *Control and cybernetics*, 35(3):599–620, 2006.
- [19] Gaston Tarry. Le problème des labyrinthes. *Nouvelles Annales de Mathématiques: Journal des candidats aux Écoles Polytechnique et Normale*, 14:187–190, 1895.
- [20] Robert Tibshirani. Regression shrinkage and selection via the lasso. *Journal of the Royal Statistical Society: Series B (Methodological)*, 58(1):267–288, 1996.
- [21] Ryan J. Tibshirani. The lasso problem and uniqueness. *Electronic Journal of Statistics*, 7:1456–1490, 2013.
- [22] Peter van Emde Boas, Robert Kaas, and Erik Zijlstra. Design and implementation of an efficient priority queue. *Mathematical Systems Theory*, 10(1):99–127, 1976.
- [23] Bernard M. Waxman. Routing of multipoint connections. *IEEE Journal on Selected Areas in Communications*, 6(9):1617–1622, 1988.
- [24] Chr Wiener. Ueber eine aufgabe aus der geometria situs. *Mathematische Annalen*, 6(1):29–30, 1873.
- [25] Winston Yap and Filip Biljecki. A global feature-rich network dataset of cities and dashboard for comprehensive urban analyses. *Scientific data*, 10(1):667, 2023.
- [26] Hangrui Yue, Qingzhi Yang, Xiangfeng Wang, and Xiaoming Yuan. Implementing the alternating direction method of multipliers for big datasets: A case study of least absolute shrinkage and selection operator. *SIAM Journal on Scientific Computing*, 40(5):A3121–A3156, 2018.